7796 J. Med. Chem. 2010, 53, 7796–7803
DOI: 10.1021/jm1009555

Journal of Medicinal Chemistry Article

Cationic Porphycenes as Potential Photosensitizers for Antimicrobial Photodynamic Therapy

Xavier Ragàs,[†,‡] David Sánchez-García,[†] Rubén Ruiz-González,[†] Tianhong Dai,[‡,⊥] Montserrat Agut,[†] Michael R. Hamblin,[‡,⊥,∥] and Santi Nonell*,[†]

[†]*Institut Químic de Sarrià, Universitat Ramon Llull, Barcelona 08017, Spain,* [‡]*Wellman Center for Photomedicine, Massachusetts General Hospital, Boston, Massachusetts 02114, United States,* [⊥]*Department of Dermatology, Harvard Medical School, Boston, Massachusetts 02115, United States, and* [∥]*Harvard-MIT Division of Health Sciences and Technology, Cambridge, Massachusetts 02139, United States*

Received July 27, 2010

Structures of typical photosensitizers used in antimicrobial photodynamic therapy are based on porphyrins, phthalocyanines, and phenothiazinium salts, with cationic charges at physiological pH values. However, derivatives of the porphycene macrocycle (a structural isomer of porphyrin) have barely been investigated as antimicrobial agents. Therefore, we report the synthesis of the first tricationic water-soluble porphycene and its basic photochemical properties. We successfully tested it for in vitro photoinactivation of different Gram-positive and Gram-negative bacteria, as well as a fungal species (*Candida*) in a drug-dose and light-dose dependent manner. We also used the cationic porphycene in vivo to treat an infection model comprising mouse third degree burns infected with a bioluminescent methicillin-resistant *Staphylococcus aureus* strain. There was a 2.6-$\log_{10}$ reduction ($p < 0.001$) of the bacterial bioluminescence for the PDT-treated group after irradiation with 180 J·cm^{-2} of red light.

Introduction

Antimicrobial photodynamic therapy (APDT[a])[1] is being actively studied as a possible alternative to antibiotic treatment for localized infections.[2,3] The basic principles are well-understood: in essence, the interaction between light and photoactive drugs, usually called photosensitizers (PSs), forms reactive oxygen species (ROS) created through either electron transfer (type I) or energy transfer (type II) reactions.[4] These ROS will react with many cellular components that will induce oxidative processes leading to cell death.[5−7]

PSs belonging to a variety of chemical structures have been used to inactivate microbial cells; most of them were porphyrin-based,[8] phthalocyanine-based,[9] or phenothiazinium-based.[10] Porphycene, a structural porphyrin isomer, is endowed with favorable photophysics that allows it to act as a photodynamic agent,[11] but has rarely been used in the field of APDT. The only two studies using polylysine−porphycene conjugates[12,13] showed promising results, but that research was not pursued, likely due to the lengthy and complex synthesis of the porphycene macrocycle available at that time needed to obtain the polymer conjugate. The recent discovery in our laboratory of a straightforward, four-step synthesis of porphycenes[14] provides an opportunity for the assessment of the potential of these compounds in APDT.

The use of outer wall-disrupting agents, such as EDTA[15] or cationic polypeptide polymixin B,[8,16] and the conjugation of the PS with polymers,[17] nanoparticles,[18] or biomolecules,[19] provides a higher affinity of the PSs against microbial cells. Nevertheless, the discovery that positively charged PSs at physiological pH values promote the photoinactivation of microbial cells[20−22] has stimulated the development of new synthetic routes to develop new useful cationic PSs for APDT. In addition, Caminos et al. showed that, in porphyrins with cationic (A) and noncationic (B) groups, the photosensitized inactivation of *E. coli* cellular suspensions with those compounds follows the order: $A_3B^{3+} > A_4^{4+} \gg ABAB^{2+} > AB_3^{+}$.[23]

In this paper, we report the synthesis of the first aryl cationic water-soluble porphycene as well as its photochemical characterization. In addition, herein we present the results of a study designed to evaluate in vitro the broad-spectrum antimicrobial efficacy of this novel light-activated PS against a panel of prototypical human pathogenic microbes, as well as its potential in vivo application to infection using a third-degree mouse burn model infected with a drug-resistant bacterial strain, methicillin-resistant *Staphylococcus aureus* (MRSA).

Experimental Section

Reagents and Solvents. 2,7,12,17-Tetrakis-(*p*-(methoxymethyl)phenyl) porphycene (**1**; MeO_4-TBPo) was prepared using previously described procedures.[14] All other reagents were purchased from Sigma-Aldrich and were used as received: HBr (33 wt % in acetic acid); pyridine (ACS reagent, ≥99.0%). Solvents used for spectroscopic measurements were spectrophotometric grade.

*Corresponding author. Phone: +34932672000. Fax: +34932056266. E-mail: santi.nonell@iqs.url.edu.

[a]Abbreviations: APDT, antimicrobial photodynamic therapy; CFU, colony forming units; DC, dark control; DMA, dimethyl acetamide; DMSO, dimethyl sulfoxide; EDTA, ethylenediamine tetraacetic acid; LC, light control; MRSA, methicillin-resistant *Staphylococcus aureus*; *m*-THPP, 5,10,15,20-tetrakis(*m*-hydroxyphenyl)-21*H*,23*H*-porphine; NTC, nontreated control; PBS, phosphate buffered saline; PDT, photodynamic therapy; PS, photosensitizer; ROS, reactive oxygen species; TMPyP, 5,10,15,20-tetrakis(*N*-methyl-4-pyridyl)-21*H*,23*H*-porphine; TPPo, 2,7,12,17-tetraphenylporphycene.

 Published on Web 10/11/2010 © 2010 American Chemical Society

Chemical Synthesis. Nuclear magnetic resonance spectra were obtained with a Varian Gemini 400HC (400 MHz ^{1}H NMR and 100.5 MHz ^{13}C NMR) equipment. Chemical shifts are expressed in ppm. For the ^{1}H NMR spectra, trimethylsilane (TMS) was used as reference. For the ^{13}C NMR spectra, the chemical shifts of the solvents (d_6-DMSO and $CDCl_3$) were used as standards. The notation for the analysis is as follows: s (singlet), d (doublet), t (triplet), q (quartet), dd (doublet of doublets), m (multiplet), sd (deuterable signal), brs. (broad signal). High-resolution mass spectra (HRMS) were registered with a Microtof (Bruker) of high-resolution (ESI-TOF technique) by the mass spectroscopy service of Universidade de Santiago de Compostela.

2,7,12-Tris(*p*-(bromomethyl)phenyl)-17-(*p*-(methoxymethyl)-phenyl) porphycene (2, Br_3MeO-TBPo). 204 mg (0.26 mmol) of MeO_4-TBPo were dissolved in 200 mL of anhydrous dichloromethane. Then, 43 mL of hydrogen bromide solution 33 wt % in acetic acid (425 mmol) were added dropwise while allowing the system to stand in a water/ice bath 3 h. Finally, the reaction mixture was diluted with 200 mL of chilled water and the organic phase was extracted with dichloromethane. The organic layer was washed with water and $NaHCO_3$ saturated solution. The organic extracts were dried over $MgSO_4$ and solvent removed under reduced pressure. The raw brominated mixture was purified through a silica pad (cyclohexane/dichloromethane; 1:1) and the desired product, that elutes the second, is isolated and washed with cyclohexane. Twenty-five milligrams of product **2** (η = 10%) were obtained as dark violet powder. ^{1}H NMR (δ/ppm, $CDCl_3$): 9.93 (s, 1H), 9.92 (s, 3H), 9.70 (s, 4H), 8.32 (d, J = 8.0 Hz, 8H), 7.85 (d, J = 8.0 Hz, 8H), 7.80 (d, 2H), 4.79 (s, 6H), 4.75 (s, 2H), 3.58 (s, 3H). ^{13}C NMR (δ/ppm, $CDCl_3$): 137.6, 136.8, 132.1, 132.0, 131.6, 131.5, 129.9, 129.4, 128.6, 74.8, 33.7, 29.9. UV/vis (toluene): 666 (46060), 631 (47100), 588 (34630), 396 (82680), 380 (102100). HRMS (ESI-TOF) m/z $C_{49}H_{37}Br_3N_4O$ calcd, 937.0550; found, 937.0578.

2,7,12-Tris(α-pyridinio-*p*-tolyl)-17-(*p*-(methoxymethyl)phenyl) porphycene (3, Py_3MeO-TBPo). Twenty-five milligrams of tribrominated Br_3MeO-TBPo were placed in a 50 mL round-bottom flask and dissolved with the minimum amount of pyridine. The solution was heated at 80 °C for 2 h and the precipitated solid recovered after centrifugation. The solid was washed with *tert*-butyl methyl ether (3 × 5 mL) and dried under vacuum. 25 mg of product **3** were obtained as a dark powder (η = 85%). The purity of **3** was confirmed by thin layer chromatography using a precoated TLC plate (silica gel C18 0.25 mm; Macherey-Nagel) in a trifluoroacetic acid/acetonitrile mixture (20:80), providing a unique spot at R_f = 0.26, and by HPLC analysis using a Lichrocart Purospher STAR RP-18E column (Supporting Information). ^{1}H NMR (δ/ppm, d_6-DMSO): 10.19 (brs, 4H), 10.05 (brs, 4H), 9.47 (d, J = 9.2 Hz, 6H), 8.76 (t, 3H), 8.50 (d, 6H), 8.40 (d, J = 8.0 Hz, 2H), 8.34 (t, 6H), 8.06 (d, J = 9.2 Hz, 6H), 7.84 (d, J = 8.0 Hz, 2H), 3.83 (t, 2H), 8.06 (d, J = 9.2 Hz, 12H), 6.18 (s, 6H), 4.72 (s, 2H), 3.83 (s, 2H), 3.49 (s, 3H). ^{13}C NMR (δ/ppm, d_6-DMSO): 146.7, 145.5, 144.7, 144.1, 143.8, 143.5, 142.7, 142.4, 142.0, 138.9, 137.0, 135.0, 134.8, 134.5, 134.1, 132.4, 131.6, 130.3, 129.1, 128.9, 125.9, 115.3, 73.9, 63.6, 58.3. UV/vis (MeOH): 656 (112200), 624 (99890), 582 (80850), 391 (190700), 375 (232400). HRMS (ESI-TOF) m/z $C_{52}H_{47}N_4O_4^{2+}$ calcd, 466.7072; found, 466.7066.

General Spectroscopic Measurements. Absorption spectra were recorded on a Cary 4E spectrophotometer (Varian, Palo Alto, CA). Absorption coefficients were derived from the slopes of Beer−Lambert plots. Fluorescence emission spectra were recorded in a Spex Fluoromax-2 spectrofluorometer (Horiba Jobin-Ybon, Edison, NJ). Fluorescence decays were recorded with a time-correlated single photon counting system (Fluotime 200, PicoQuant GmbH, Berlin, Germany) equipped with a red sensitive photomultiplier. Excitation was achieved by means of a 375 nm picosecond diode laser working at 10 MHz repetition rate. The counting frequency was always below 1%. Fluorescence lifetimes were analyzed using PicoQuant *FluoFit 4.0* data analysis software. Transient absorption spectra were monitored by nanosecond laser flash photolysis using a Q-switched Nd:YAG laser (Surelite I-10, Continuum) with right-angle geometry and an analyzing beam produced by a Xe lamp (PTI, 75 W) in combination with a dual-grating monochromator (mod. 101, PTI) coupled to a photomultiplier (Hamamatsu R928). Kinetic analysis of the individual transients was performed with software developed in our laboratory.

$^1O_2$ phosphorescence was detected by means of a customized PicoQuant Fluotime 200 system described in detail elsewhere.[24] $^1O_2$ signal amplitudes were determined by analysis of the data using the *FluoFit 4.0* software.

All spectroscopic measurements were carried out in 1 cm quartz cuvettes (Hellma, Germany) at room temperature.

Microbial Strains and Culture Conditions. The microorganisms studied were *Staphylococcus aureus* 8325-4, methicilin-resistant *S. aureus* Xen 31 (a kind gift from Xenogen Corp, Alameida, CA), and *Enterococcus faecalis* (ATCC29212) as Gram-positive bacteria; *Acinetobacter baumanii* (ATCC 51393), *Escherichia coli* (ATCC 53868), *Proteus mirabilis* (ATCC 51393), and *Pseudomonas aeruginosa* (ATCC 19660) as Gram-negative bacteria; and *Candida albicans* (ATCC 18804) and *C. krusei* (ATCC 6258) as yeasts.

Bacteria were aerobically grown overnight at 37 °C in an orbital shaking incubator at 130 rpm in brain-heart infusion (BHI) broth (Fischer Scientific) to stationary phase, and an aliquot was then grown in fresh BHI medium at 37 °C to an Abs_{600} = 0.5, corresponding to ca. 10^8 colony forming units (CFU)/mL (logarithmic phase). The suspensions were then centrifuged (5 min, 3500 rpm) and resuspended with sterile PBS at pH 7.4 at the same concentration for phototoxicity experiments. *C. albicans* was grown overnight at 30 °C in yeast peptone dextrose (YPD) broth (Fischer Scientific), centrifuged (5 min, 3500 rpm), and resuspended with sterile PBS at pH 7.4 up to ca. 10^7 CFU/mL for phototoxicity experiments. *C. krusei* was grown overnight at 35 °C in Sabouraud broth (Merck) and then grown in new Sabouraud medium at 35 °C in an orbital shaking incubator at 130 rpm to an Abs_{600} = 0.7, corresponding to ca. 10^7 CFU/mL. The suspensions were then centrifuged (5 min, 3500 rpm) and resuspended with sterile PBS at pH 7.4 at the same concentration for phototoxicity experiments.

Light Sources. All bacterial suspensions and *C. albicans* were irradiated with a 652 ± 15 nm light delivered by a noncoherent light source (LumaCare, Newport Beach, CA), an optical fiber bundle, and a lens (to form a 2-cm-diameter spot) using a 125 mW·cm^{-2} fluence rate. *C. krusei* was irradiated by means of a Sorisa Photocare at 635 ± 10 nm using a 35 mW·cm^{-2} fluence rate. Fluence rates were routinely measured using a power meter (Coherent, Portland, OR).

Photodynamic Inactivation Studies. Suspensions of bacteria (10^8 CFU/mL) or yeast (10^7 CFU/mL) in PBS were incubated in the dark at room temperature for 30 min with increasing concentrations of the PS (added from 5 mM dimethylacetamide (DMA) stock solution). Centrifugation (3 min, 12 000 rpm) of 1 mL aliquots was used to remove the excess of PS that was not taken up by the microbial cells when experiments required it. Then, 1 mL aliquots of the cell suspensions were placed in 24 well plates. The wells were illuminated from the top of the plates by use of red light and fluences ranged from 0 to 100 J·cm^{-2}. At times during the illumination when the requisite fluences had been delivered, aliquots were taken from each well (the suspensions were thoroughly mixed before sampling to avoid the settlement of cells). For determination of CFU, the aliquot was serially diluted, streaked on nutrient agar, and incubated in the dark for 18 h at 37 or 30 °C. Experiments were carried out in triplicate for each condition. Controls using the same amount of organic solvent, in the presence of the porphycene and without light, and with light alone, were performed for all experimental conditions, obtaining less than 1-$\log_{10}$ reduction in bacterial viability in all cases.

Photodynamic Inactivation in a Burn Infected Mouse Model. Adult female BALB/c mice (Charles River Laboratories,

Scheme 1

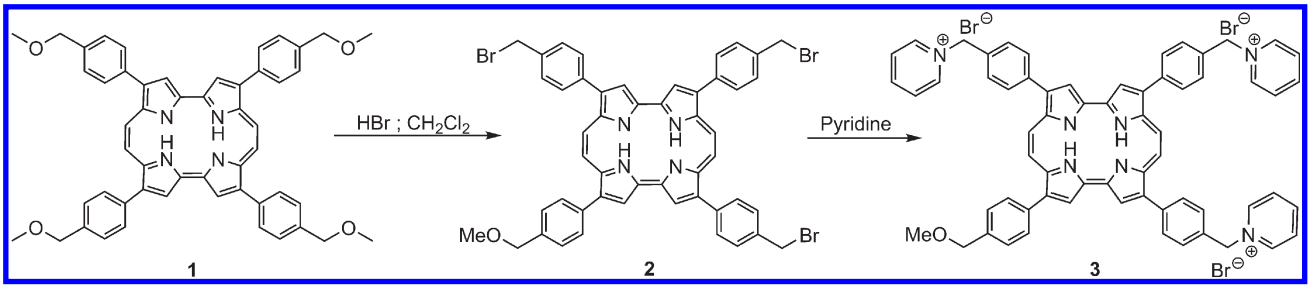

Wilmington, MA), 6−8 week old and weighing 17−21 g, were used in the study. The animals were housed one per cage and maintained on a 12 h light/dark cycle with access to food and water ad libitum. All animal procedures were approved by the Subcommittee on Research Animal Care (IACUC) of Massachusetts General Hospital and met the guidelines of National Institutes of Health. Twenty mice were randomly divided into four groups of five animals each; these groups were designated (A) PDT; (B) PS dark control; (C) light alone control; (D) no treatment control. In vivo experiments were performed in burn infections by means of the protocol used by Dai et al. fully described elsewhere.[25] Briefly, bacterial infection took place as described by Ha et al.[26] Five minutes after the creation of burns (to allow the burns to cool down), a suspension (50 μL) of bacteria in sterile PBS containing 10^8 cells was inoculated onto the surface of each burn with a pipet tip and then was smeared onto the burn surface with an inoculating loop. The bioluminescence imaging system (Hamamatsu Photonics KK, Bridgewater, NJ) has been described elsewhere in detail.[27] Briefly, an ICCD photon-counting camera (model C2400−30H; Hamamatsu Photonics, Bridgewater, NJ) was used. The camera was mounted in a light-tight specimen chamber fitted with a light-emitting diode, a setup that allowed for a background gray-scale image of the entire mouse to be captured. By accumulating many images containing binary photon information (an integration time of 2 min was used), a pseudocolor luminescence image was generated. Superimposition of this image onto the gray-scale background image yielded information on the location and intensity in terms of photon number. The camera was also connected to a computer system through an image processor (Argus-50, Hamamatsu Photonics). Argus-50 control program (Hamamatsu Photonics) was used to acquire images and to process the image data collected. The mice were imaged immediately after applying the bacteria to ensure that the bacterial inoculum applied to each burn was consistent.

Thirty minutes after the infection, 50 μL of porphycene solution (10% dimethylsulfoxide in PBS) were added to groups A and B and 30 min was allowed for the PS to bind to and penetrate the bacteria. Then, mice were again imaged to quantify any dark toxicity to the bacteria. Mice (groups A and C) were then illuminated with 652 ± 15 nm light delivered by a noncoherent light source with a power density of 100 mW·cm^{-2}. Mice were given total light doses of 180 J·cm^{-2} in aliquots with bioluminescence imaging taking place after each aliquot of light. Immediately after PDT, mice in all groups were resuscitated with an IP injection of 0.5 mL sterile saline to prevent dehydration.

Statistics. Survival fractions are expressed as means ± standard error of the mean (SEM) of three independent experiments. Differences between the killing curves were evaluated by means of paired Student's t test. Differences between three or more means were compared by a one-way ANOVA. P values of <0.05 were considered significant.

Results

Synthesis. Treatment of prophycene **1** with HBr (33% in acetic acid) in dichloromethane[27] furnishes a mixture of brominated porphycenes resulting from the substitution of methoxy groups with bromine atoms at the benzylic positions. From this mixture, mainly inseparable dibrominated derivatives, the tribrominated porphycene **2** can be isolated easily by column chromatography. Finally, heating of porphycene **2** in pyridine as a solvent provides the corresponding pure tribromide **3** (Py_3MeO-TBPo·Br_3)[28,29] as a deep blue precipitate (Scheme 1). Purity of **3** was determined by multiple methods including (low-resolution) laser desorption mass spectrometry, (high-resolution) electrospray mass spectrometry, ^{1}H and ^{13}C NMR spectroscopy, UV−visible absorption spectroscopy, fluorescence spectroscopy, HPLC analysis, and reverse-phase thin-layer chromatography (Supporting Information). In all cases, the purity was estimated to be >95%.

Table 1. Photophysical Properties of Py_3MeO-TBPo

solvent	λ_{abs} / nm	λ_f / nm	Φ_f [a]	τ_S / ns	τ_T / μs[b]	k_q / M^{-1} s^{-1}[c]	Φ_Δ (λ_{ex} / nm)[d]
H_2O	644	656	0.005	1.8	330	1.5×10^9	0.03 (355) 0.004 (532)
MeOH	655	661	0.075	2.6	152	3.5×10^9	0.193

[a] Cresol violet was used as reference. [b] Lifetime of the decays at 420 nm in argon-saturated solutions. [c] Rate constant for triplet quenching by oxygen. Error bar 10%. [d] Singlet oxygen quantum yield in air-saturated solutions. Excitation wavelength in parentheses.

Physical and Photophysical Properties. The photophysical properties of Py_3MeO-TBPo are summarized in Table 1. As observed in Figure 1, Py_3MeO-TBPo shows the typical porphycene absorption spectrum in MeOH, with three bands in the red range of the spectrum and absorption coefficients in the 50.000 M^{-1} cm^{-1} range. The spectrum in water loses much of the structure, indicating not surprisingly that aggregation is occurring in aqueous media despite the three positive charges. The extent of aggregation can be controlled by changing the ionic strength of the solution, i.e., the compound is substantially more aggregated in PBS than in pure water. However, both in aqueous solvents and in MeOH the fluorescence emission spectra match the typical fluorescence spectrum of porphycenes, where a main band and a weaker shoulder at lower energies are observed that are the mirror image of the $S_1 \leftarrow S_0$ absorption transition[11] Interestingly, the fluorescence excitation spectrum matches in all cases the absorption spectrum of the monomer, indicating that the aggregates are not emissive.

The fluorescence quantum yield, Φ_F, was determined by comparing the integrated fluorescence intensity of the porphycene to that of an optically matched solution of cresol violet in MeOH as reference ($\Phi_F = 0.54$).[30] A value of $\Phi_F = 0.075 \pm 0.005$ was found in MeOH, while in water, the results showed a marked dependence on the excitation wavelength, reflecting the fraction of monomers that were excited at each wavelength (Supporting Information). The fluorescence

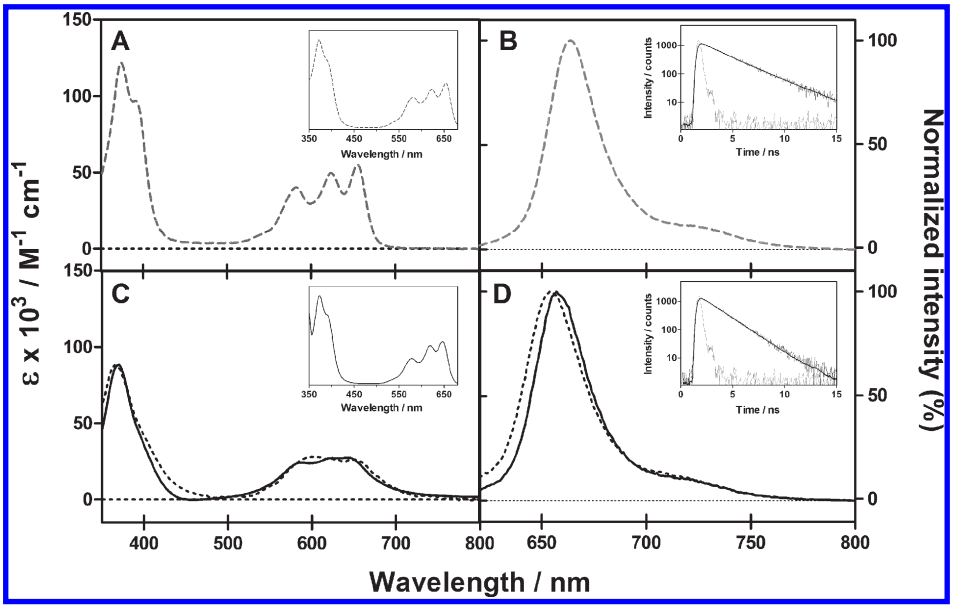

Figure 1. (A,C) Absorption and (B,D) fluorescence spectrum of Py_3MeO-TBPo in (A,B) MeOH and (C,D) water and PBS (solid and dotted line, respectively). Insets: (A,C) Excitation spectrum of the fluorescence at 661 nm. (B,D) Time-resolved fluorescence of Py_3MeO-TBPo. Signal, fit, and instrument response function at 661 nm upon excitation at 375 nm.

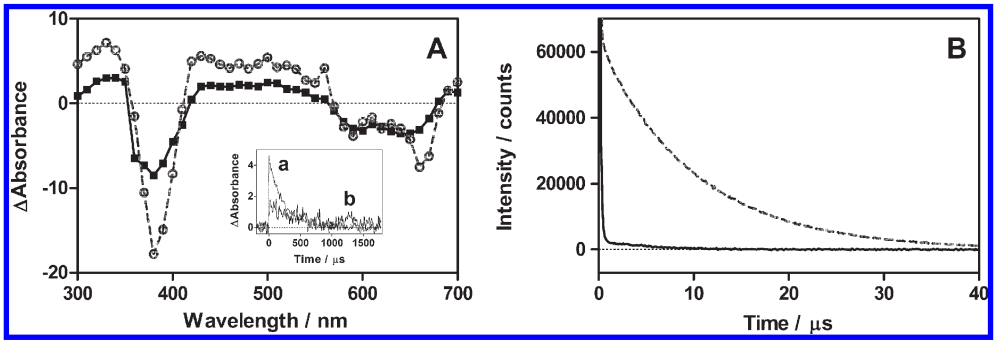

Figure 2. (A) Transient absorption spectrum of the triplet excited state of porphycence **3** in MeOH (gray, dashed line) and water (black, solid line). Inset: Transient absorbance at 420 nm upon excitation at 355 nm in (a) MeOH and (b) water. (B) Singlet oxygen phosphorescence kinetics at 1270 nm of an aqueous solution (solid line) and MeOH solution (dashed line) of Py_3MeO-TBPo.

decay was monoexponential in both solvents (Figure 1B,D), with lifetimes 1.8 ± 0.1 ns in water and 2.6 ± 0.1 ns in MeOH. This is consistent with the similar excitation spectra and confirms that only the monomers are emissive.

Transient absorption spectra of Py_3MeO-TBPo in argon atmosphere are shown in Figure 2. Again, they present a shape similar to that of the triplet-minus-singlet spectrum of tetraphenylporphycene (TPPo), confirming that only the monomeric species can undergo intersystem crossing.[31] The decays at 420 nm show a triplet lifetime of 330 μs in water and 152 μs in MeOH, with rate constants of oxygen quenching (k_q) of 1.5×10^9 $M^{-1} \cdot s^{-1}$ and 3.5×10^9 $M^{-1} \cdot s^{-1}$, respectively.

The singlet oxygen ($^1O_2$) production quantum yield, Φ_Δ, was determined by means of its phosphorescence at 1270 nm (Figure 2B), comparing the intensity of the $^1O_2$ signal shown by the porphycene to that of optically matched solutions of reference PSs.[32] Using *m*-tetrahydroxyphenylporphine (*m*-THPP) and tetra-*N*-methylpyridylporphine (TMPyP) as standards ($\Phi_\Delta^{ref} = 0.69$ and 0.74, respectively),[33,34] Φ_Δ values of 0.004 ± 0.001 and 0.19 ± 0.01 were determined in water and MeOH, respectively, upon excitation at 532 nm. While in MeOH the Φ_Δ values were independent of the excitation wavelength, we obtained $\Phi_\Delta = 0.03 \pm 0.01$ in water upon excitation at 355 nm using sulfonated phenalenone as standard ($\Phi_\Delta^{ref} \sim 1$).[35] It can thus be concluded that the photophysical properties of **3** in MeOH are very similar to those of typical tetraphenylporphycenes,[11] while in aqueous media, aggregation strongly prevents its photosensitizing ability. This finding is fully in line with the results of decades of research on related tetrapyrrole macrocycles.

In Vitro Photoinactivation of Bacteria. All Gram-positive tested species were completely eliminated (no colonies observed) by PDT in a porphycene-concentration (Figure 3A) and energy-dose (Supporting Information) dependent manner. *E. faecalis* was the most sensitive species to Py_3MeO-TBPo-PDT showing 6-$\log_{10}$ reduction in bacterial viability with a 0.5 μM porphycene concentration and an energy dose of 30 $J \cdot cm^{-2}$. 1 μM or 2 μM porphycene concentration and 15 $J \cdot cm^{-2}$ were needed, respectively, to produce a similar effect for *S. aureus* and MRSA in a porphycene-concentration and energy dose-dependent manner.

Gram-negative species could be similarly inactivated (Figure 3B and Supporting Information), although higher concentrations and light doses were needed. For instance, 8 μM of **3** and 100 $J \cdot cm^{-2}$ were needed to induce a 6-$\log_{10}$

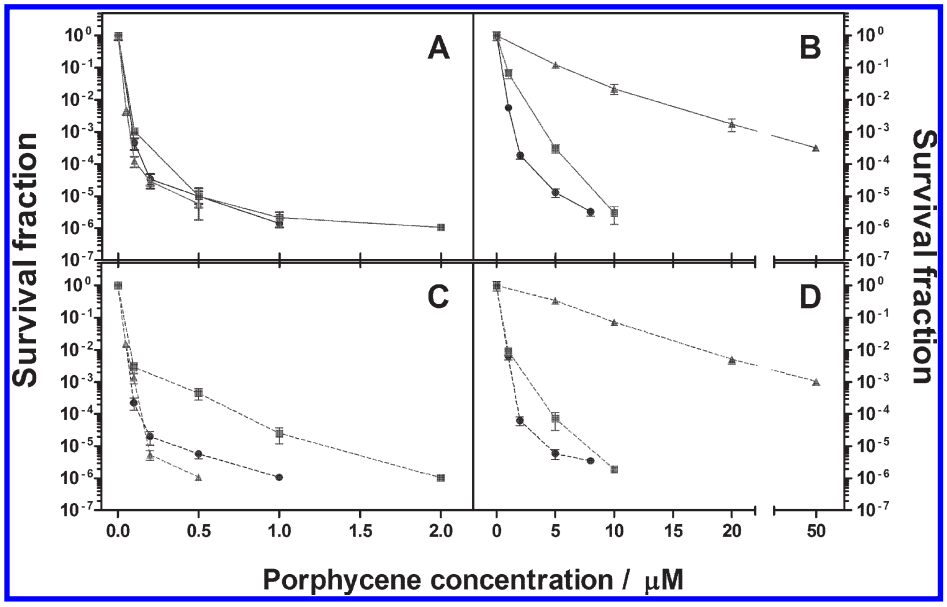

Figure 3. Bacterial photoinactivation with Py_3MeO-TBPo. (A,C) Survival curves of MRSA (squares), *S. aureus* (circles), and *E. faecalis* (triangles) with (dashed line) and without (solid line) removing the excess of photosensitizer (PS) from the solution after 30 J·cm^{-2} of 652 nm light. (B,D) Survival curves of *A. baumanii* (circles), *E. coli* (squares), and *P. mirabilis* (triangles) with (dashed line) and without (solid line) removing the excess of PS from the solution after 60 J·cm^{-2} (*E. coli*) and 100 J·cm^{-2} (*A. baumanii* and *P. mirabilis*) of 652 nm light.

reduction in the bacterial viability for *A. baumanii*, while 10 μM and 60 J·cm^{-2} were needed in the case of *E. coli*. Only a modest 3-log$_{10}$ reduction in the survival fraction was achieved for *P. mirabilis* even at 50 μM and 100 J·cm^{-2}, and no relevant inactivation (< 1-log$_{10}$ reduction in the survival fraction) could be observed for *P. aeruginosa* even at 100 μM porphycene concentration and light dose of 100 J·cm^{-2}.

All the inactivation curves were performed with and without removal of the excess of PS (Figure 3C,D). No significant statistical difference was obtained in any case ($P > 0.26$). This finding implied that the porphycene displayed strong binding to the bacterial cells.

In Vitro Photoinactivation of Yeasts. *Candida* species are generally used in APDT as representative models of fungal cells as they grow as single cell suspensions. Both species were completely eliminated by Py_3MeO-TBPo in a concentration-dependent (Figure 4) and light dose-dependent manner (Supporting Information), irrespective of the removal of the porphycene excess from the solution. As observed in the figure, while 50 μM concentration of Py_3MeO-TBPo and 30 J·cm^{-2} were needed to obtain a 5-log$_{10}$ reduction in the cell viability of *C. albicans*, only 10 μM concentration and 15 J·cm^{-2} proved necessary to produce the same reduction in the cell viability of *C. krusei*. Removing the excess of PS did not produce any significant difference ($P = 0.75$).

In Vivo Photoinactivation of MRSA in Infected Burns. Bioluminescent MRSA (Xen31) has a stably integrated lux operon that has been optimized for expression in Gram-positive bacteria[36] and leads to spontaneous light emission at 37 °C in the absence of any exogenously added substrate. It has been previously demonstrated that MRSA CFUs quantified using serial dilutions of bacterial suspensions correlate linearly with the bioluminescence emitted by those bacteria.[36]

Figure 5A shows the successive bioluminescence images obtained from four representative mouse burns (from groups A, B, C, and D) infected with MRSA. The burn treated with

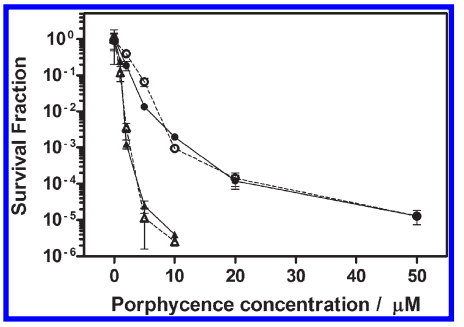

Figure 4. Yeast photoinactivation with Py_3MeO-TBPo. Survival curves of *C. albicans* (circles) after 30 J·cm^{-2} of 652 nm light and *C. krusei* (triangles) after 15 J·cm^{-2} of 635 nm light, with (dashed line) and without (solid line) removal of the excess of photosensitizer (PS) from the solution.

PDT received 100 μM of Py_3MeO-TBPo and 652 nm light up to 180 J·cm^{-2}; the dark control burn received the same amount of porphycene and no light; while the light-alone burn received 652 nm light up to 180 J·cm^{-2} and no porphycene. A nontreated control burn received neither PS nor light. A complete elimination of the bioluminescence signal was observed in the PDT-treated burn after a light dose of 180 J·cm^{-2} in the presence of Py_3MeO-TBPo.

The light-dose responses of normalized mean bioluminescence values ($n = 5$) of the different mouse groups are shown in Figure 5B. PDT induced a reduction of ca. 2.6-log$_{10}$ of the bioluminescence, while less than 0.3-log$_{10}$ reduction was observed for all the control groups. The statistical analysis at each energy dose by 1-factor ANOVA test showed significant differences among all the control groups and the PDT-treated group ($P < 0.001$).

Discussion

A potential PS for APDT must have appropriate photophysical properties, such as a large long-wavelength absorption band and a high quantum yield for the generation of both

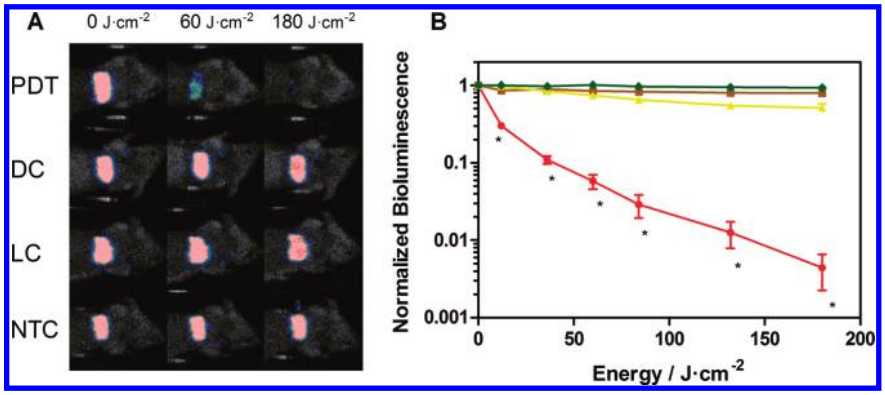

Figure 5. In vivo MRSA photoinactivation with Py_3MeO-TBPo. (A) Dose response of bacterial luminescence from burns infected with luminescent MRSA and treated with 100 μM of porphycene **3** and 652 nm light (PDT), with 100 μM of Py_3MeO-TBPo only (DC), with light (LC) only, and without treatment (NTC). (B) Light-dose response curves of the normalized bioluminescence for mice treated with photodynamic therapy (red), mice treated only with Py_3MeO-TBPo (brown), mice treated only with light (yellow), and mice without treatment (green). Every point is an average of five independent mice. *, $P < 0.001$.

long-lived triplet excited state and cytotoxic ROS species. It also has to be water-soluble and must have a high affinity for microbial cells and a low affinity for host cells, characteristics that are strongly related to the presence of cationic charges in the molecular structure.

As observed in the absorption spectrum and despite the cationic charges, Py_3MeO-TBPo is soluble although aggregated in water, which deteriorates its photophysical properties. The differential behavior in aqueous and more lipophilic environments may be valuable for unmistakably ascertaining the localization of the porphycene bound to the cells by means of fluorescence microscopy. From the point of view of APDT applications, it can be expected that Py_3MeO-TBPo would be a good PS if binding to microbial cells prevents its aggregation. Conversely, any nonbound PS will be aggregated and thus will not be able to cause photodamage to surrounding tissue. The fact that the absorption spectrum of the aggregates shows lower absorption coefficients is also an advantage, as these nonbound molecules will see their light-filtering ability reduced. The presence of aggregates can also be observed in the Φ_F and Φ_Δ values in water. For instance, as observed in Table 1, the Φ_Δ drops from 0.03 to 0.004 when changing the excitation wavelength. This change is due to the different absorption coefficient ratio monomer/aggregates at both wavelengths. At 355 nm, the ratio is higher, leading to a lower light-filtering effect, i.e., to a higher Φ_Δ. The different trend observed in the lifetime values of the singlet (τ_s) and triplet (τ_T) excited states can be explained by two different factors. On one hand, the presence of aggregates in H_2O enables a new deactivation pathway by intermolecular interactions of the porphycene molecules, leading to a decrease in the τ_s value. In comparison to TPPo (τ_T = 4.8 ns in toluene),[37] τ_s in MeOH is lower, probably due to the higher degrees of freedom of the residues bound to the porphycene ring. On the other hand, the triplet excited-state population is basically controlled by the oxygen concentration in the solutions ($k_q \approx 10^9$ M^{-1} s^{-1}). Thus, despite the measurements having been performed in argon-saturated solutions, the solubility of oxygen in H_2O is lower than in MeOH, i.e., the remaining amount of oxygen molecules in the solutions is lower, leading then to a longer τ_T value. As regards k_q, the values are in the range of those observed in diffusion-controlled quenching reactions, and the reduction observed in H_2O, relative to that in MeOH, is due to the higher viscosity of water.

Concerning the in vitro PDT experiments with Gram-positive bacteria, it was observed that low concentrations of porphycene (< 2 μM), as well as low light doses (< 30 J·cm^{-2}), were enough to completely eliminate all the strains. On the other hand, because of the generally higher resistance of Gram-negative species,[16] higher light doses (> 60 J·cm^{-2}) were needed in order to inactivate the Gram-negative bacterial strains tested with somewhat larger PS concentrations (< 10 μM). However, neither high concentrations of porphycene nor high light doses were able to completely eliminate *P. mirabilis* or significantly inactivate *P. aeruginosa*. A possible reason for the different susceptibility within Gram-positive bacterial strains is the difference in antioxidant enzyme levels. As for Gram-negative bacteria, a possible explanation can be the different membrane permeability among *A. baumanii* (high), *E. coli* (intermediate), and *P. mirabilis* (low).

Consistent with the photophysics results, there are no significant differences between the inactivation curves recorded in the presence or absence of the excess PS ($P > 0.26$), suggesting a high lipophilicity of the porphycene, i.e., a high-affinity against bacterial cells, which indicates that only the PS bound to the cells is involved in the photodynamic effect. Thus, according to the classification of PSs established by Deminova and Hamblin,[17] the porphycene might be tightly bound to the microbial cell and might be able to penetrate into microorganisms, as happened when poly(L-lysine) chlorin(e6) conjugate was used as PS.

As for the yeast studies, *Candida* species were selected as the model to study the activity of porphycenes against fungal cells. Our data show that porphycenes can be used as a valuable alternative to typical antifungal PSs, as they are able to completely inactivate both *C. albicans* and *C. krusei* using lower light doses and lower porphycene concentrations than for currently used PSs.[17,38−40]

Despite the optimal properties of the porphycene in vitro, its value as PS must be further assessed from experiments in vivo.

DMA was used as in vitro stock solution because it does not quench hydroxyl radicals. However, PBS with DMSO was used as in vivo stock solution instead of DMA because DMSO helps the penetration of the dye into the infected tissue. The tests in burns infected with MRSA demonstrate that porphycenes can clearly produce statistically significant differences between the controls and the PDT-treated group ($P < 0.001$), reducing by 2.6-$\log_{10}$ units the bioluminescence of MRSA in an energy-dose dependent manner upon irradiation with 180 J·cm^{-2} and a porphycene concentration of 100 μM.

These results compare favorably to those obtained by Dai et al.,[41] where a 2.7-$\log_{10}$ reduction of the bioluminescence signal was obtained in a skin abrasion wound infected with MRSA by using polyethylenimine-chlorin(e6) conjugate and 660 nm red light and by Zolfaghari et al.,[42] where 1.4-$\log_{10}$ and 1.15-$\log_{10}$ where obtained in excision and superficial scarified wounds treated with methylene blue and 670 nm red light, respectively.

Conclusions

The synthetic availability of cationic porphycenes, as well as their optimal physical and photophysical properties, suggests the porphycene-core macrocycle can be a potentially interesting antimicrobial PS. The demonstrated high photodynamic activity against a broad-spectrum of microbial cells in vitro as well as an in vivo infection model supports the further scrutiny of this family of compounds.

Acknowledgment. This work was supported by a grant of the Spanish Ministerio de Ciencia e Innovación (CTQ2007-67763-C03-01/BQU) and by U.S. NIH grant R01AI050875 to MRH. X.R. and R.R. were supported by the Generalitat de Catalunya (DURSI) and Fons Social Europeu with a predoctoral fellowship. R.R. also thanks Obra Social "la Caixa" for its Master's grant. T.D. was supported by the Bullock-Wellman Postdoctoral Fellowship Award. We thank Sorisa for providing us with the Sorisa Photocare LED source and Xenogen Corp for the gift of XEN31.

Supporting Information Available: ^{1}H NMR and ^{13}C NMR spectra of porphycenes **2** and **3**. HPLC analysis of porphycene **3**. Figures of the calculation of the fluorescence quantum yields and energy-dose experiments for in vitro photodynamic inactivation. Methodology for the calculation of singlet oxygen quantum yields.This material is available free of charge via the Internet at http://pubs.acs.org.

References

(1) Wainwright, M. Photodynamic antimicrobial chemotherapy (PACT). *J. Antimicrob. Chemother.* **1998**, *42*, 13–28.
(2) Wainwright, M. Photoantimicrobials--so what's stopping us? *Photodiagn. Photodyn. Ther.* **2009**, *6*, 167–169.
(3) Dai, T.; Huang, Y. Y.; Hamblin, M. R. Photodynamic therapy for localized infections--state of the art. *Photodiagn. Photodyn. Ther.* **2009**, *6*, 170–188.
(4) Schweitzer, C.; Schmidt, R. Physical mechanisms of generation and deactivation of singlet oxygen. *Chem. Rev.* **2003**, *103*, 1685–1757.
(5) Michaeli, A.; Feitelson, J. Reactivity of singlet oxygen toward amino acids and peptides. *Photochem. Photobiol.* **1994**, *59* (3), 284–289.
(6) Stark, G. Functional consequences of oxidative membrane damage. *J. Membr. Biol.* **2005**, *205*, 1–16.
(7) Ravanat, J. L.; Di Mascio, P.; Martinez, G. R.; Medeiros, M. H. G.; Cadet, J. Singlet oxygen induces oxidation of cellular DNA. *J. Biol. Chem.* **2000**, *275*, 40601–40604.
(8) Nitzan, Y.; Gutterman, M.; Malik, Z.; Ehrenberg, B. Inactivation of Gram-Negative Bacteria by Photosensitized Porphyrins. *Photochem. Photobiol.* **1992**, *55*, 89–96.
(9) Bertoloni, G.; Rossi, F.; Valduga, G.; Jori, G.; Ali, H.; Vanlier, J. E. Photosensitizing activity of water-soluble and lipid-soluble phthalocyanines on prokaryotic and eukaryotic microbial-cells. *Microbios* **1992**, *71*, 33–46.
(10) Romanova, N. A.; Brovko, L. Y.; Moore, L.; Pometun, E.; Savitsky, A. P.; Ugarova, N. N.; Griffiths, M. W. Assessment of photodynamic destruction of *Escherichia coli* O157: H7 and *Listeria monocytogenes* by using ATP bioluminescence. *Appl. Environ. Microbiol.* **2003**, *69*, 6393–6398.
(11) Stockert, J. C.; Canete, M.; Juarranz, A.; Villanueva, A.; Horobin, R. W.; Borrell, J.; Teixido, J.; Nonell, S. Porphycenes: Facts and prospects in photodynamic therapy of cancer. *Curr. Med. Chem.* **2007**, *14*, 997–1026.
(12) Polo, L.; Segalla, A.; Bertoloni, G.; Jori, G.; Schaffner, K.; Reddi, E. Polylysine-porphycene conjugates as efficient photosensitizers for the inactivation of microbial pathogens. *J. Photochem. Photobiol., B* **2000**, *59*, 152–158.
(13) Lauro, F. M.; Pretto, P.; Covolo, L.; Jori, G.; Bertoloni, G. Photoinactivation of bacterial strains involved in periodontal diseases sensitized by porphycene-polylysine conjugates. *Photochem. Photobiol. Sci.* **2002**, *1*, 468–470.
(14) Sanchez-Garcia, D.; Borrell, J. I.; Nonell, S. One-pot synthesis of substituted 2,2′-bipyrroles. A straightforward route to aryl porphycenes. *Org. Lett.* **2009**, *11*, 77–79.
(15) Bertoloni, G.; Rossi, F.; Valduga, G.; Jori, G.; Vanlier, J. Photosensitizing activity of water-soluble and lipid-soluble phthalocyanines on *Escherichia coli*. *FEMS Microbiol. Lett.* **1990**, *71*, 149–155.
(16) Malik, Z.; Ladan, H.; Nitzan, Y. Photodynamic inactivation of gram-negative bacteria - Problems and possible solutions. *J. Photochem. Photobiol., B* **1992**, *14*, 262–266.
(17) Demidova, T. N.; Hamblin, M. R. Effect of cell-photo sensitizer binding and cell density on microbial photoinactivation. *Antimicrob. Agents Chemother.* **2005**, *49*, 2329–2335.
(18) Guo, Y. Y.; Rogelj, S.; Zhang, P. Rose bengal-decorated silica nanoparticles as photosensitizers for inactivation of gram-positive bacteria. *Nanotechnology* **2010**, *21*.
(19) Friedberg, J. S.; Tompkins, R. G.; Rakestraw, S. L.; Warren, S. W.; Fischman, A. J.; Yarmush, M. L. Antibody-targeted photolysis - bacteriocidal effects of Sn (IV) chlorin e6- Dextran-monoclonal antibody conjugates. *Ann. N.Y. Acad. Sci.* **1991**, *618*, 383–393.
(20) Minnock, A.; Vernon, D. I.; Schofield, J.; Griffiths, J.; Parish, J. H.; Brown, S. B. Photoinactivation of bacteria. Use of a cationic water-soluble zinc phthalocyanine to photoinactivate both gram-negative and gram-positive bacteria. *J. Photochem. Photobiol., B* **1996**, *32*, 159–164.
(21) Merchat, M.; Bertolini, G.; Giacomini, P.; Villanueva, A.; Jori, G. Meso-substituted cationic porphyrins as efficient photosensitizers of gram-positive and gram-negative bacteria. *J. Photochem. Photobiol., B* **1996**, *32*, 153–157.
(22) Wainwright, M.; Phoenix, D. A.; Marland, J.; Wareing, D. R. A.; Bolton, F. J. A study of photobactericidal activity in the phenothiazinium series. *FEMS Immunol. Med. Microbiol.* **1997**, *19*, 75–80.
(23) Caminos, D. A.; Spesia, M. B.; Durantini, E. N. Photodynamic inactivation of *Escherichia coli* by novel meso-substituted porphyrins by 4-(3-*N,N,N*-trimethylammoniumpropoxy)phenyl and 4-(trifluoromethyl)phenyl groups. *Photochem. Photobiol. Sci.* **2006**, *5*, 56–65.
(24) Jimenez-Banzo, A.; Ragas, X.; Kapusta, P.; Nonell, S. Time-resolved methods in biophysics. 7. Photon counting vs. analog time-resolved singlet oxygen phosphorescence detection. *Photochem. Photobiol. Sci.* **2008**, *7*, 1003–1010.
(25) Dai, T. H.; Tegos, G. P.; Lu, Z. S.; Huang, L. Y.; Zhiyentayev, T.; Franklin, M. J.; Baer, D. G.; Hamblin, M. R. Photodynamic therapy for *Acinetobacter baumannii* burn infections in mice. *Antimicrob. Agents Chemother.* **2009**, *53*, 3929–3934.
(26) Ha, U. W.; Jin, S. G. Expression of the soxR gene of *Pseudomonas aeruginosa* is inducible during infection of burn wounds in mice and is required to cause efficient bacteremia. *Infect. Immunol.* **1999**, *67*, 5324–5331.
(27) Hamblin, M. R.; O'Donnell, D. A.; Murthy, N.; Contag, C. H.; Hasan, T. Rapid control of wound infections by targeted photodynamic therapy monitored by in vivo bioluminescence imaging. *Photochem. Photobiol.* **2002**, *75*, 51–57.
(28) Yamashita, T.; Uno, T.; Ishikawa, Y. Stabilization of guanine quadruplex DNA by the binding of porphyrins with cationic side arms. *Bioorg. Med. Chem.* **2005**, *13*, 2423–2430.
(29) Ikawa, Y.; Moriyama, S.; Harada, H.; Furuta, H. Acid-base properties and DNA-binding of water soluble *N*-confused porphyrins with cationic side-arms. *Org. Biomol. Chem.* **2008**, *6*, 4157–4166.
(30) Magde, D.; Brannon, J. H.; Cremers, T. L.; Olmsted, J. Absolute luminescence yield of cresyl violet - Standard for the red. *J. Phys. Chem.* **1979**, *83*, 696–699.
(31) Rubio, N.; Borrell, J. I.; Teixido, J.; Canete, M.; Juarranz, A.; Villanueva, A.; Stockert, J. C.; Nonell, S. Photochemical production and characterisation of the radical ions of tetraphenylporphycenes. *Photochem. Photobiol. Sci.* **2006**, *5*, 376–380.
(32) Nonell, S.; Braslavsky, S. E. *Methods in Enzimology*; Academic Press: London, 2000; pp 1−682.
(33) Wilkinson, F.; Helman, W. P.; Ross, A. B. Quantum yields for the photosensitized formation of the lowest electronically excited singlet state of molecular oxygen in solution. *J. Phys. Chem. Ref. Data* **1993**, *22*, 113–262.

(34) Redmond, R. W.; Gamlin, J. N. A compilation of singlet oxygen yields from biologically relevant molecules. *Photochem. Photobiol.* **1999**, *70*, 391–475.
(35) Nonell, S.; Gonzalez, M.; Trull, F. R. 1*H*-Phenalen-1-One-2-Sulfonic Acid - An extremely efficient singlet molecular-oxygen sensitizer for aqueous-media. *Afinidad* **1993**, *50*, 445–450.
(36) Francis, K. P.; Joh, D.; Bellinger-Kawahara, C.; Hawkinson, M. J.; Purchio, T. F.; Contag, P. R. Monitoring bioluminescent *Staphylococcus aureus* infections in living mice using a novel luxABCDE construct. *Infect. Immunol.* **2000**, *68*, 3594–3600.
(37) Rubio, N.; Prat, F.; Bou, N.; Borrell, J. I.; Teixido, J.; Villanueva, A.; Juarranz, A.; Canete, M.; Stockert, J. C.; Nonell, S. A comparison between the photophysical and photosensitising properties of tetraphenyl porphycenes and porphyrins. *New J. Chem.* **2005**, *29*, 378–384.
(38) Foley, J. W.; Song, X. Z.; Demidova, T. N.; Jilal, F.; Hamblin, M. R. Synthesis and properties of benzo[a]phenoxazinium chalcogen analogues as novel broad-spectrum antimicrobial photosensitizers. *J. Med. Chem.* **2006**, *49*, 5291–5299.
(39) Zeina, B.; Greenman, J.; Purcell, W. M.; Das, B. Killing of cutaneous microbial species by photodynamic therapy. *Br. J. Dermatol.* **2001**, *144*, 274–278.
(40) Codling, C. E.; Maillard, J. Y.; Russell, A. D. Aspects of the antimicrobial mechanisms of action of a polyquaternium and an amidoamine. *J. Antimicrob. Chemother.* **2003**, *51*, 1153–1158.
(41) Dai, T.; Tegos, G. P.; Zhiyentayev, T.; Mylonakis, E.; Hamblin, M. R. Photodynamic therapy for methicillin-resistant *Staphylococcus aureus* infection in a mouse skin abrasion model. *Lasers Surg. Med.* **2010**, *42*, 38–44.
(42) Zolfaghari, P. S.; Packer, S.; Singer, M.; Nair, S. P.; Bennett, J.; Street, C.; Wilson, M. *In vivo* killing of *Staphylococcus aureus* using a light-activated antimicrobial agent. *BMC Microbiol.* **2009**, *9*, 27.